

Cohesion and Adhesion Interlayer of the Thermal Barrier Coatings Made of Cobalt Alloy MAR-M509

Z. A. Opiekun^{a*}, A. Trytek^a

^aDepartment of Casting and Welding, Rzeszów University of Technology Al. Powstańców Warszawy 12, 35-959 Rzeszów, Poland

*Corresponding autor; e-mail: zopiekun@gmail.com

Received 31.03.2014; accepted in revised form 14.04.2014

Abstract

The manuscript presents microstructure, geometrical product specification and results of scratch tests performed on the interlayer of thermal barrier coating (TBC) with Rockwell's intender. The TBC was provided by depositing two layers; metallic interlayer and external ceramic layer onto a plate coating made of cobalt alloy MAR-M509 in plasma spraying process. The surface of the casting was sandblasted with Al_2O_3 powder in an air stream before the TBC was introduced. Scratches were made along the cross-section from a mould material (MAR-M509) through metallic interlayer and external ceramic layer in the TBC. Friction force, friction factor and acoustic emission were recorded during the test. It has been proved that metallic interlayer in the TBC of ca. 200 μm thickness forms tough coating without pores with good cohesion values and very good adhesion values to the mould.

Keywords: Cobalt alloy MAR-M509, Geometrical product specification (GPS), Thermal barrier coating (TBC), Interlayer cohesion, Adhesion, Scratch test

1. Introduction

Thermal barrier coatings (TBC) are applied via plasma spraying technology (APS – Air Plasma System) and build up usually with two layers: metallic interlayer and external ceramic layer [1-3]. For special purposes when high density of coating and its good bonding with the mould is demanded the TBC is applied in vacuum plasma spraying process (VPS – Vacuum Plasma Spray) or low pressure plasma spraying technique (LPPS – Low Pressure Plasma Spray) [4]. The TBC has an excellent heat resistance and a small thermal conductivity. They are characterized by an erosion and abrasion resistance and resistance to aggressive chemicals [5]. Therefore, the TBC are becoming more commonly used as coatings of jet-propelled parts of aircraft engines (combustor, BOAS – Blade Outer Air Seal, blades of turbine), valves and parts in chemical reactors [6-7].

On the metallic interlayers are usually applied materials with MeCrAlY group single oxides belong to ceramic materials which are most often used on the external layer in the TBC; Al_2O_3 , ZrO_2 , ThO_2 , BeO , MgO , CeO_2 , Cr_2O_3 i Y_2O_3 [5]. Thermal barrier coatings are the layers which separate the surface of metallic material from the stream of hot gases. Simultaneously they reduce the temperature of metallic items [8]. In the end, such an influence of the TBC causes an improvement of performance characteristic of jet turbine engine, a reduction of fuel consumption, an increase of inlet gas temperature (ca. 100-170°C) and a decrease of toxic substance emission from outlet gases because of better fuel consumption [7].

ZrO_2 oxide stabilized by Y_2O_3 is most often used for the external layer in the TBC [9-12]. Functional properties, adhesion, cohesion and crack resistance depends on a phase composition of this oxide. Solid solutions prepared on the basis

of regular ZrO_2 (C) are low resistant to changeable heat load. Considerable improvement of crack resistance of these solutions is noticed at presence of tetragonal phase of ZrO_2 (T) in the TBC. Factors which favour the tetragonal phase in the TBC after cooling down to the room temperature from the temperature of plasma spraying, are small ZrO_2 -8% Y_2O_3 irregular grain sizes and introduction of about 8 wt% of Y_2O_3 to the solid solution of ZrO_2 - Y_2O_3 [3,13,14].

The aim of this article is an attempt at describing the cohesion and adhesion metallic interlayer made of 45%Ni-22%Co-17%Cr-16%Al alloy, and presenting the geometrical product specification of the ceramic external layer made of ZrO_2 oxides deposited on the casting of plate made of MAR-M509 cobalt alloy. The coating was obtained by single spraying metallic powder made of 45%Ni-22%Co-17%Cr-16%Al-0,3%Y alloy and triple spraying ceramic powder made of ZrO_2 - 8% Y_2O_3 oxides onto the surface of the casting with a MultiCoat Plasma Coating System² (Sulzer Metco).

2. Material and methodology of testing

Plate castings made of cobalt alloy MAR-M509 of dimension 4x20x90 mm were used for tests. The composition of plates was as follow: 0,60%C; 28,83%Cr; 10,0%Ni; 7,12%W; 3,77%Ta; 0,36%Zr; 0,18%Ti; 0,007%B; 0,43%Fe; 0,02%Mn; 0,03%Si; 0,002%S; rest: Co. The plates were casted in the multilayer ceramic mould (MCM) at initial temperature ca. 1000°C. The liquid alloy MAR-M509 at temperature ca. 1495±5 °C [15,16] was poured over MCM in a medium-frequency induction vacuum furnace. The surface of plate castings was at first sandblasted with Al_2O_3 powder of 200÷250 µm grain diameter in an air stream of pressure ca. 0.35MPa for a few seconds. After single layer of 45%Ni-22%Co-17%Cr-16%Al-0,3Y powder alloy was covered and next triple layers of ZrO_2 - 8% Y_2O_3 powder oxides in an argon-hydrogen plasma beam. The plates were to heat at temperature about 120°C before covered layers.

Two spray powders were used in the experiment: one 45%Ni-22%Co-17%Cr-16%Al-0,3Y powder alloy, fine spherical morphology with particle granulation, ca. 75±15 µm and ZrO_2 - Y_2O_3 oxide powder which shows irregular morphology with particle granulation, ca. 53±15 µm.

A deposition of all layers in the TBC was done using: primary plasma gas, Ar (40 l/min), secondary plasma gas, H_2 (10 l/min), electric current about 600 A, powder feet rate (40 g/min), spray distance about 130 mm, traverse speed of a spraying gun was constant at 2 mm/min and also constant speed of rotated holder (60 rot/min). The state of surface of plate castings was assessed with the Talyscan 150 (Taylor-Hobson) tool working with the Mountains Map Universal program before and after the ceramic layers was deposited. Six amplitude parameters of geometrical product specification (GPS) were analysed: S_a (arithmetic mean), S_z (mean of the 5 highest peaks and the 5 lowest points), S_t (total height), S_q (quadratic mean), S_p (highest peak over the mean), S_v (lowest valley under the mean).

X-ray examination surface of the TBC was performed with the Siemens Kristalloflex D500 X-ray diffractometer.

The examination of cohesion and adhesion of the TBC was carried out with the Revetest Scratch Tester CSM Instruments tool. The surface of sample with the TBC was scratched with the diamond Rockwell's intender of a 200 µm top radius. During the test, six different forces were applied: 2, 4, 8, 16, 32 and 40 N onto the surface of a cross-section: MAR-M509 mould and TBC. It has been assumed that each scratch is 0.5 mm long. In the interlayer of the TBC and in the MAR-M509 mould, scratches were made at a 5 N intender load along 0.5 mm. All scratches were made at a rate of 1 mm/min - the speed of the intender. The Revetest Scratch Tester tool was calibrated according to reference sample covered with TiN coating. Friction force, friction factor and acoustic emission were recorded during the test. 100% of acoustic emission scale equals to 65 dB value.

3. Results

3.1. Geometrical structure of a surface

Geometrical product specification (GPS) and surface load-capacity curve of external ceramic layer in the TBC presented in figure 1.

3.2. Microstructure and X-ray diffraction pattern

Microstructure of the plate casting made of alloy MAR-M509 with the TBC at the cross-section is presented in figure 2. The X-ray diffraction patterns of the external ceramic layer in the TBC surface are shown in figure 3.

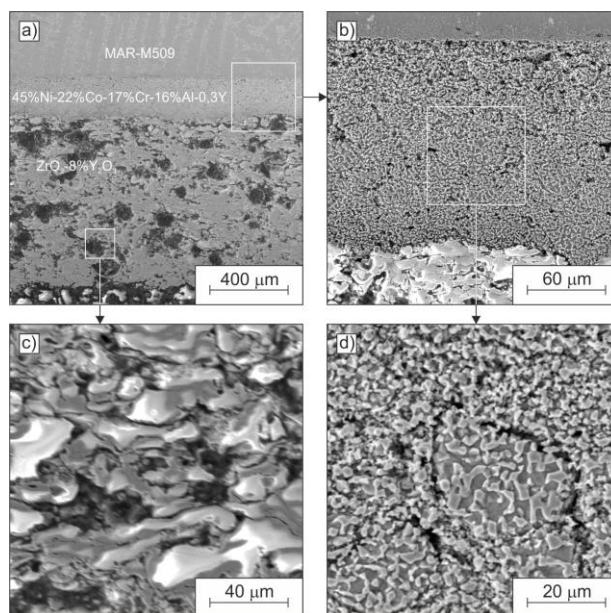


Fig. 2. Microstructure at the cross-section: mould (MAR-M509) - coating (TBC) (a, b), external ceramic layer (ZrO_2) (c), metallic interlayer (45%Ni-22%Co-17%Cr-16%Al-0,3%Y) (d), SEM micrograph

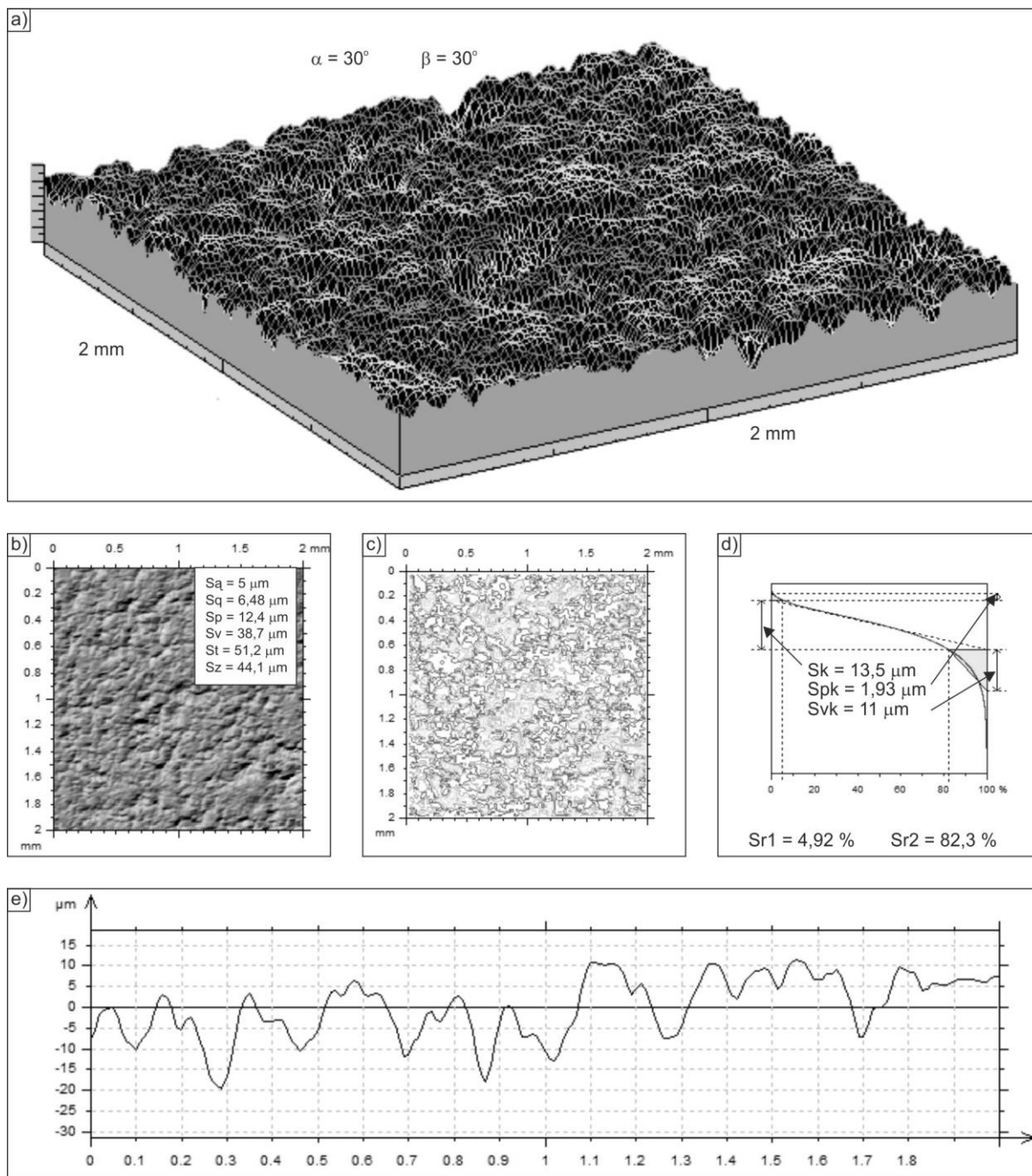


Fig. 1. Surface topography of the external ceramic layer in the TBC. 3D view (a), plate surface with amplitude parameters (b), coating map (c), load-capacity curve of GPS and its parameters d), surface profile e), geometrical parameters S_k , S_{pk} , S_{vk} , S_{r1} , S_{r2}

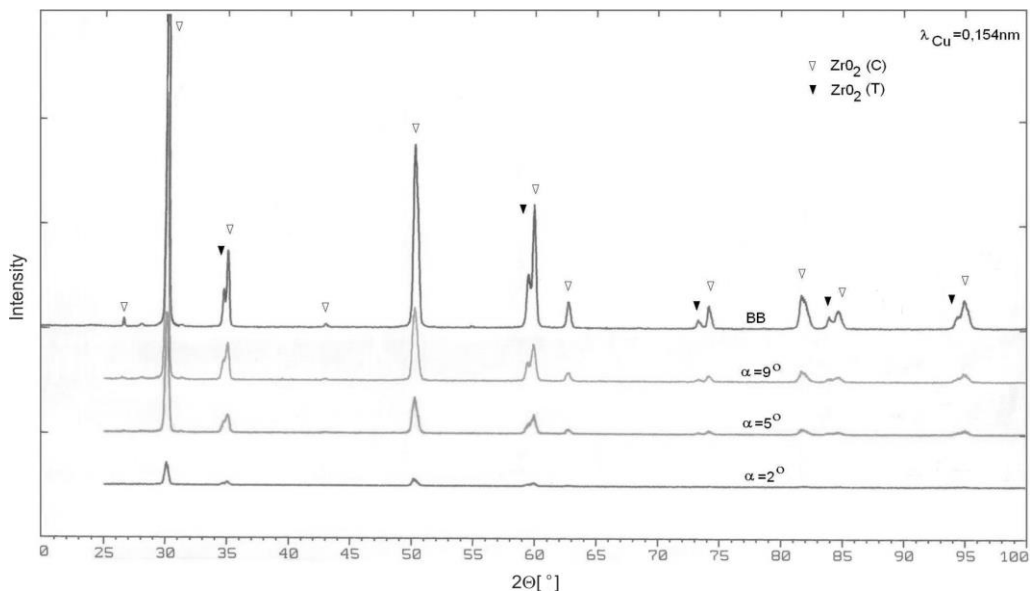


Fig. 3. Diffraction patterns of the external ceramic layer in the TBC surface obtained for a grazing incident geometry $\alpha = 2, 5$ and 9° and in the Bragg-Brentano geometry (BB). ZrO_2 (C) – regular, ZrO_2 (T) – tetragonal

3.3. Cohesion and adhesion

The control scratched with the diamond Rockwell's indenter made of onto the surface of a cross-section MAR-M509 mould and TBC (fig. 4).

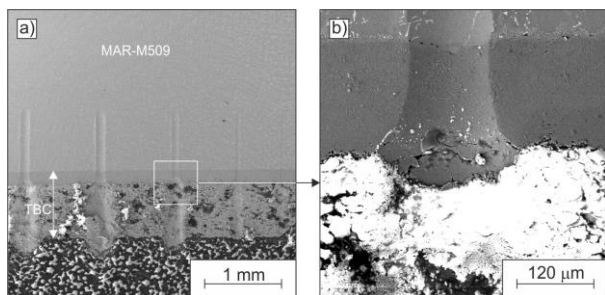


Fig. 4. Macrostructure with the picture of surface scratches (a), example of the scratch Rocwell's indenter for the a loading force 8N of a cross-section; MAR-M509 mould, metallic interlayer (45%Ni-22%Co-17% Cr-16%Al-0,3%Y) and external ceramic layer (ZrO_2 -8% Y_2O_3) (b), SEM micrograph

The pictures of surface scratches at the cross-section: mould (MAR-M509) – metallic interlayer 45%Ni-22%Co-17%Cr-16%Al-0,3%Y in the TBC together with diagrams of friction force, friction factor and acoustic emission changes are presented in figure 5.)

The scratches of samples in the direction from the mould (MAR-M509 cobalt alloy) through the metallic interlayer in the TBC at the cross-section, which are made at constant indenter loads, reveal the presence of typical plastic strain cones (fig. 5b), crack cones in the coating (fig. 5a) and “pushes-P” of mould material into this interlayer. The surfaces of longitudinal sections of A_{ca} cones, which characterise the cohesion of the

interlayer, are described by a product $l_x \cdot l_y$ (fig. 5b) [17] and are plotted as a function of loading force (fig. 6). The “pushes” of mould material into a metallic interlayer and lack of cracks at a boundary: mould – interlayer (fig. 5) indicate a very good interlayer adhesion to the mould.

4. Summary

The coating of the TBC of ca. 920 μm thickness was obtained as a result of spraying melted powder made of 45%Ni-22%Co-17% Cr-16%Al-0,3Y alloy and ceramic powder made of ZrO_2 -8% Y_2O_3 oxides the surface of a plate casting made of the MAR-M509 cobalt alloy in a plasma beam (Fig. 2). Such a coating consists of a two layers fine grain metallic interlayer 45%Ni-22%Co-17% Cr-16%Al-0,3Y of, ca. 200 μm thickness and external ceramic layer as a mixture of two phases, regular ZrO_2 (C) and tetragonal ZrO_2 (T) (Fig.3). The microstructure of the metallic interlayer in the TBC is tough, homogeneous and deprived of porosity (total porosity less than 2%) (Fig. 2b,c). The metallic interlayer was deposited on the plate surface which was activated by sandblasting with Al_2O_3 particles and to heat at temperature about 120°C. The geometrical product specification (GPS) of the sandblasted plate is isotropic. Its amplitude parameters S_a , S_q , S_p , S_v , S_t and S_z are 3,1 μm , 3,9 μm , 16,2 μm , 18,3 μm , 34,5 μm and 31,4 μm respectively and functional parameters S_k , S_{pk} , S_{vk} , S_{r1} , S_{r2} are 10 μm , 4,0 μm , 3,5 μm , 9,6% and 91,4% respectively. The GPS of the external ceramic layer in the TBC is also isotropic but it is rougher than the mould. A total height S_t of the layer has increased by ca. 50% and an arithmetic mean S_a by ca. 60% in comparison to S_t and S_a for sandblasted surface of the mould. A roughness of the core (S_k) has increased by ca. 35%. The only functional parameter of GPS of ceramic layer which is lower by ca. 100% in comparison to the mould is a roughness of peaks (S_{pk}) (Fig. 1).

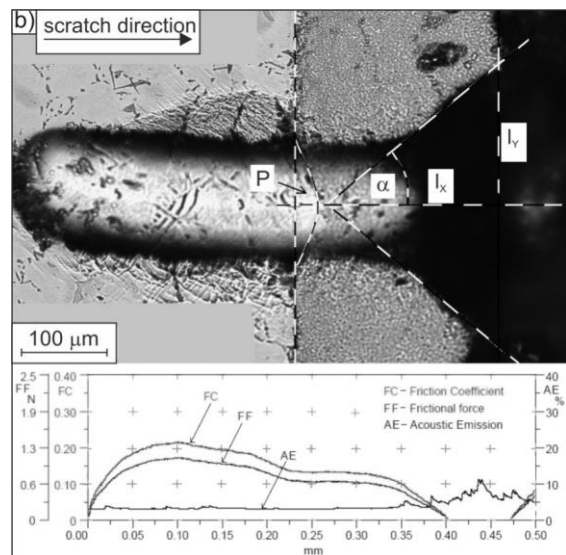
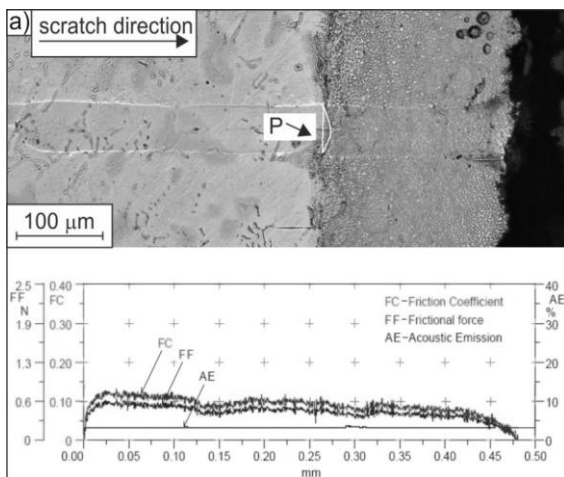


Fig. 5. Examples of scratches along the cross-section: mould (MAR-M509 - interlayer (45%Ni-22%Co-17% Cr-16%Al-0,3%Y) in the TBC, together with diagrams of friction force, friction coefficient and acoustic emission changes for a loading force 4N a), 32N b)

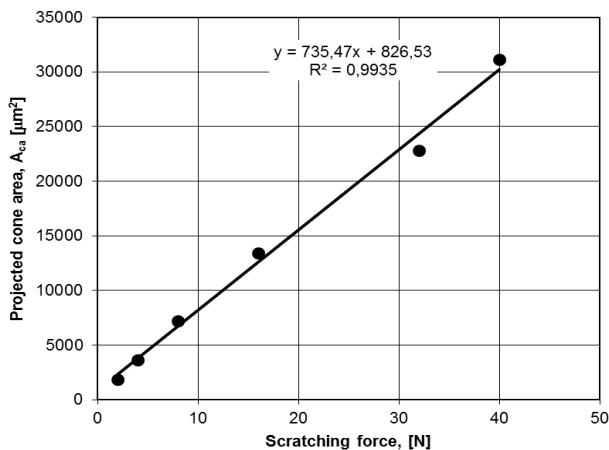


Fig. 6. Surfaces of longitudinal sections of A_{ca} cones plotted as a function of loading force in the metallic interlayer 45%Ni-22%Co-17% Cr-16%Al-0,3Y

The scratches of samples along the cross-section from the mould (MAR-M509 cobalt alloy) through the metallic interlayer and external ceramic layer (fig. 4a,b) in the TBC, which were made with Rockwell's cone at different intender loads (fig. 5a,b), reveal the presence of typical strain and crack cones in the interlayer and "pushes-P" of mould material (γ phase) into the interlayer. A linear surface increase of longitudinal sections of these cones indicates good cohesion of metallic interlayer (Fig. 6).

A load increase of the Rockwell's intender from 2N to 40N causes an increase of friction force from ca. 0.3N to 10N together with a minor increase of friction coefficient from ca. 0.1 to 0.2. For all scratches, no increase of acoustic emission effect is observed at boundary mould-coating. The constant value of acoustic emission at 3% level (ca. 2 dB) shows that strains at boundary MAR-M509 cobalt alloy – metallic

interlayer in the TBC are plastic and do not appear in this crack area. The shape of "pushes" of γ phase is similar to the cones and its depth increases linearly together with the increase of intender loading force from ca. 3 μ m for 2N force to ca. 53 μ m for 40N force. Such a course of changes happening at boundary mould (MAR-M509 cobalt alloy), metallic interlayer in the TBC during an attempt at scratching, proves a very good adhesion this interlayer made of 45%Ni-22%Co-17% Cr-16%Al-0,3% alloy.

Cracks in "cohesion cones" of the metallic interlayer in the TBC are noticed when the loading force of the intender exceeds 16N. Huge differences (even 6.5 dB) between values of acoustic emission are the effect of the interlayer cracking (fig. 5b).

Acknowledgements

1. The equipment was purchased under the project „Creation, development and modernisation of the scientific and research base of the Rzeszów University of Technology" within the framework of the Podkarpackie Voivodeship Regional Operational Programme for the years 2007-2013.
2. The apparatus was purchased under the project No. POPW.01.03.00-18-012/09 from Structural Funds provided in the framework of the Operational Programme 'Development of Eastern Poland' co-funded by the European Unions from the European Regional Development Fund

References

- [1] Pint B. A., Wright J. G., Bridlley W.J.: Evaluation of TBC systems on novel substrates. Journal of Thermal Spray Technology, 9 (6) (2000), 198-203
- [2] Parks W.P.Jr, Hoffman E.E., Lee W.Y. Wright J.G.: Thermal barrier coatings issue in advanced land –based turbines. Journal of Thermal Spray Technology, 6 (2) (1997), 187-192

- [3] Pint B.A., Wright I.G., Lee W.Y. Zhang Y., Prussner K., Aleksander K.B.: Substrate and bond coat compositions. Factory affecting alumina scale adhesion. *Materials Science Engineering*, A245 (1998), 201-211
- [4] Davis J. R.: *Handbook of thermal spray technology* ASM. International Materials Park, 2004
- [5] Gugel E., Woetting G. G.: Materials selection for ceramic components in automobiles. *Industrial Ceramics*, 19 (1999), 196-199
- [6] Masayuki Arai: Damage Assessment of TBC Sprayed Combustor of Land – Based Gas Turbine, *Journal of the Society of Materials Science, Japan*, Vol. 57, No.3 (2008), 285-291
- [7] Jordan E. H., Gell M.: Solution precursor plasma spray of thermal barrier coatings. *Advanced coatings for high temperatures. Processing Turbine Forum, Nicea 2008*
- [8] Stover D., Funke C.: Direction of the development of thermal barrier coatings in energy applications. *Journal of Material Processing Technology*, (92-93) (1999), 152-202
- [9] Coderet Y.: Development of high temperature coatings and TBC bond coats for gas turbine engines. *Advanced coatings for high temperatures. Processing Turbine Forum, Nicea 2008*
- [10] Ballard D. J., Schadler L. S., Levis C., Devenport J.: Phase transformation in thermal barrier coatings. *Rensselaer Polytechnic Institute Research Experience for Undergraduates*, 2000
- [11] Bach W. F., Babiak Z., Duda T., Copitzky T., Josefiak L. A.: Thermal barrier coatings with enhanced properties - A chance for thermal spraying. *United Thermal Spray Conference, Dusseldorf 1999*
- [12] Miller A. R.: Thermal barrier coatings for aircraft engines. History and directions, *Journal of Thermal Spray Technology*, (6) (1997), 3
- [13] Haberko K., Pampuch R.,: Influence of yttrium content on phase composition and mechanical properties of Y-TZP. *Ceramics International* (9) (1983), 8-12
- [14] Viancenzini P.: Zirconia thermal barrier coatings for engine application. *Industrial Ceramics* (10) (1990) 3, 113-126
- [15] Opiekun Z.: Analysis of process-related factors that determine structure and properties of cobalt casting alloy intended of aircraft part. *Monograph, Poznań 2007*
- [16] Opiekun Z.: Temperature influence of ceramic form on the structure of cobalt alloy MAR-M509 castings, *Acta Metallurgica Sinica (English Letters)*, vol. 24, nr 1, 23-33, 2011
- [17] CSM Instruments, *Application Bulletin: Characterization of thermal spray coatings by instrumented indentation and scratch testing. Part I*, No. 28, 2009